Passive Energy-based Control via Energy Tanks and Release Valve for Limit Cycle and Compliance Control

Gianluca Garofalo * **Christian Ott** *

* *Institute of Robotics and Mechatronics, German Aerospace Center (DLR), Wessling, Germany (e-mail: gianluca.garofalo(at)dlr.de).*

Abstract: The problem of generating periodic solutions for a fully actuated robot is considered in this work. The result is achieved by extending the concept of limit cycle control via energy regulation, in order to guarantee passivity of the closed-loop system. Such a feature is particularly relevant in case of physical interaction with the environment, since a non-passive system could cause problems in terms of stability, robustness and safety. As energy-based limit cycle control can be used also for regulation control, the paper extends as well recent results in passivation of projection-based null space compliance control to the case of adjustable maximum allowed activity in the system.

Keywords: Force and compliance control; Passivity; Energy regulation; Limit cycles; Humanoid robots.

1. INTRODUCTION

Several challenging dynamic tasks that robots are required to solve nowadays can be described as periodic tasks, e.g. running, walking, object manipulation and crank turning in McGeer (1990); Geyer et al. (2006); Garofalo et al. (2012); Petrič et al. (2014). This is often the case whenever it is more important to stay on a prescribed orbit in the state space, rather than following the exact position in time along the desired curve. For these applications tracking a trajectory might not be the best solution, as already addressed in Westervelt et al. (2007). The need to control the energy for periodic locomotion shown in Garofalo et al. (2012), has inspired Garofalo et al. (2013); Garofalo and Ott (2016, 2017) to propose many different feedback control laws in order to produce asymptotically stable closed orbits both for rigidly and elastically actuated robots. Nevertheless, these control laws do not guaratuee the passivity of the system with respect to the external forces and the collocated velocities. This is a key point in view of recent findings in Stramigioli (2015), formally proving that passivity is a necessary requirment to ensure stable interaction with any passive environment. In pursuing an era in which robots physically interact with their environment and with humans, such a requirement becomes of paramount importance. Since Garofalo and Ott (2019) applies the energy-based limit cycle control for locomotion (interaction between the robot and the floor) and Garofalo and Ott (2016) uses it for human-robot interaction, in this work the necessary modification for the passivation of the controller is considered.

Related works are Li and Horowitz (2001); Duindam and Stramigioli (2003); Taniguchi and Fujimoto (2009); Canudas-de-Wit et al. (2002). Compared to Canudas-de-Wit et al. (2002), in the energy-based limit cycle control the solution of the problem is based on the nullspace decomposition introduced in Park et al. (1999). In this way, the controller takes advantage of the dynamic properties of the system and does not completely alter its original dynamics through feedback linearization. While Li and Horowitz (2001); Duindam and Stramigioli (2003); Taniguchi and Fujimoto (2009) force the system to follow a close integral curve of a vector field via passive control actions, here the limit cycle in the state space is obtained by regulating an energy function on a submanifold of the configuration space, as it is conceptually sketched in Fig. 1. Additionally, relating the input to the energy in the system allowed Garofalo and Ott (2017) to extend the method to elastic actuators. This energy function consists of the physical kinetic energy and a potential energy. The latter represents an additional design element in the controller for rigid actuation, while it is the physical potential energy for compliant actuation; see Garofalo and Ott (2017).

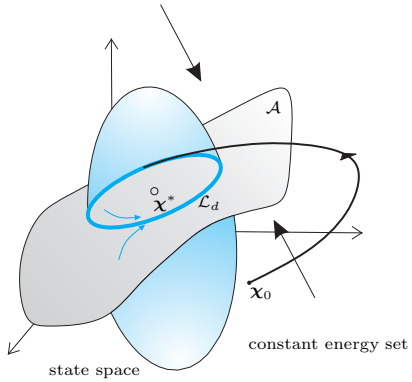

Fig. 1. Conceptual illustration of the main idea of the energy-based limit cycle controllers. The limit cycle $\mathcal{L}_d$ is generated regulating an energy function, after that the system has been forced to evolve on a submanifold $\mathcal{A}$ of the state space.

As energy-base limit cycle control is a generalization of regulation control (because setting the desired energy to zero makes the limit cycle collapse into an equilibrium point), the paper extends as well recent results in passivation of projection-based nullspace compliance control found in Dietrich et al. (2016). Switching from a positive desired energy to zero desired energy, the controller can be used for limit cycle control or compliance control.

The contributions of the paper are summarized in the following. Firstly, the passivation of projection-based null space compliance control is reformulated and additional modifications are made to guarantee the finite-time convergence of the auxiliary variables and a better numerical conditioning of the tank dynamics, guaranteeing that no energy in the tank remains unused. Secondly, the maximum level of activity allowed in the system is made adjustable, by adding the equivalent of a release valve to the energy tank. Finally, the results are extended for limit cycle control, providing a passive method to produce periodic behaviors in a robotic system.

The paper is organized as follows. Section 2 presents notation and model. In Section 3, the passivation of projection-based null space compliace control is reviewed and then modified in Section 4. Section 5 introduces the passive energy-based control for limit cycle and compliance control. Section 6 collects simulations and experimental results. Finally, Section 7 summarizes the work.

2. NOTATION AND MODEL

The considered robotic systems are modeled by the nonlinear differential equations:

$$\boldsymbol{M}(\boldsymbol{q})\ddot{\boldsymbol{q}} + \boldsymbol{C}(\boldsymbol{q},\dot{\boldsymbol{q}})\dot{\boldsymbol{q}} + \boldsymbol{g}(\boldsymbol{q}) = \boldsymbol{\tau} + \boldsymbol{\tau}_e \ , \tag{1}$$

where $\boldsymbol{q}, \dot{\boldsymbol{q}} \in \mathbb{R}^n$ (n is the number of joints) are the link positions and velocities, which constitute together the state of the robot. It is used $\boldsymbol{M} \in \mathbb{R}^{n\times n}$ to denote the symmetric and positive definite inertia matrix, $\boldsymbol{C} \in \mathbb{R}^{n\times n}$ a Coriolis matrix satisfying $\dot{\boldsymbol{M}} = \boldsymbol{C} + \boldsymbol{C}^T$ and $\boldsymbol{g} \in \mathbb{R}^n$ the gravity torque vector. Altogether they will be referred to as dynamic matrices. The torques $\boldsymbol{\tau} \in \mathbb{R}^n$ produced by the motors are an input to the system, together with the external torques $\boldsymbol{\tau}_e \in \mathbb{R}^n$.

Finally, the notation $\lfloor \boldsymbol{z} \rceil^p = |\boldsymbol{z}|^p \operatorname{sgn}(\boldsymbol{z})$ is used for a variable $\boldsymbol{z} \in \mathbb{R}^n$ and a scalar $p \in \mathbb{R}$, where the operators have to be understood as acting on each components of $\boldsymbol{z}$.

2.1 Coordinate transformation

The main task that the robot has to execute is given by a function $\boldsymbol{x} = \boldsymbol{x}(\boldsymbol{q})$ and it provides the configuration in which the robot will produce the periodic motion when the limit cycle control is used. Given $m < n$, the Jacobian matrix $\boldsymbol{J}(\boldsymbol{q}) \in \mathbb{R}^{m\times n}$ of the mapping $\boldsymbol{x} : \mathbb{R}^n \to \mathbb{R}^m$ is assumed to have full rank. This allows to rewrite the dynamics of the system with a new set of coordinates, as in Park et al. (1999); Ott et al. (2008). First, a null space base matrix $\boldsymbol{Z}(\boldsymbol{q}) \in \mathbb{R}^{(n-m)\times n}$ is computed [1], which allows to obtain the directions orthogonal to the submanifold, then $\boldsymbol{Z}(\boldsymbol{q})$ is used to compute a dynamically consistent [2] null space map $\boldsymbol{N}(\boldsymbol{q}) \in \mathbb{R}^{(n-m)\times n}$, which will be part of the extended Jacobian matrix $\boldsymbol{J}_N(\boldsymbol{q}) \in \mathbb{R}^{n\times n}$, such that

$$\begin{bmatrix}\dot{\boldsymbol{x}}\\ \boldsymbol{v}\end{bmatrix} = \boldsymbol{J}_N(\boldsymbol{q})\dot{\boldsymbol{q}} = \begin{bmatrix}\boldsymbol{J}(\boldsymbol{q})\\ \boldsymbol{N}(\boldsymbol{q})\end{bmatrix}\dot{\boldsymbol{q}} \ , \tag{2}$$

where $\boldsymbol{N}(\boldsymbol{q}) = \Big(\boldsymbol{Z}(\boldsymbol{q})\boldsymbol{M}(\boldsymbol{q})\boldsymbol{Z}^T(\boldsymbol{q})\Big)^{-1}\boldsymbol{Z}(\boldsymbol{q})\boldsymbol{M}(\boldsymbol{q})$ and $\boldsymbol{v}$ are additional null space velocities, i.e. describing the motion of the robot that does not interfere with the main task. One can show that by this choice the extended Jacobian $\boldsymbol{J}_N(\boldsymbol{q})$ is non singular and the inverse is

$$\boldsymbol{J}_N^{-1}(\boldsymbol{q}) = \begin{bmatrix}\boldsymbol{J}^{+_M}(\boldsymbol{q}) & \boldsymbol{Z}^T(\boldsymbol{q})\end{bmatrix} \ , \tag{3}$$

where $\boldsymbol{J}^{+_M}(\boldsymbol{q})$ denotes the dynamically consistent weighted pseudo inverse defined as

$$\boldsymbol{J}^{+_M}(\boldsymbol{q}) = \boldsymbol{M}^{-1}(\boldsymbol{q})\boldsymbol{J}^T(\boldsymbol{q})\Big(\boldsymbol{J}(\boldsymbol{q})\boldsymbol{M}^{-1}(\boldsymbol{q})\boldsymbol{J}^T(\boldsymbol{q})\Big)^{-1} \ . \tag{4}$$

The joint velocity can thus be computed from the Cartesian velocity and the null space velocity via

$$\dot{\boldsymbol{q}} = \boldsymbol{J}^{+_M}(\boldsymbol{q})\dot{\boldsymbol{x}} + \boldsymbol{Z}^T(\boldsymbol{q})\boldsymbol{v} \ . \tag{5}$$

From (2) and (5) it is straightforward to rewrite (1) in the extended velocity coordinates as

$$\boldsymbol{\Lambda}(\boldsymbol{q})\begin{bmatrix}\ddot{\boldsymbol{x}}\\ \dot{\boldsymbol{v}}\end{bmatrix} + \boldsymbol{\Gamma}(\boldsymbol{q},\dot{\boldsymbol{q}})\begin{bmatrix}\dot{\boldsymbol{x}}\\ \boldsymbol{v}\end{bmatrix} = \boldsymbol{J}_N^{-T}(\boldsymbol{q})\Big(\boldsymbol{\tau} + \boldsymbol{\tau}_e - \boldsymbol{g}(\boldsymbol{q})\Big) \ , \tag{6}$$

with the matrices [3] $\boldsymbol{\Lambda}(\boldsymbol{q})$ and $\boldsymbol{\Gamma}(\boldsymbol{q},\dot{\boldsymbol{q}})$ given in Ott et al. (2008) and having the notably structure

$$\boldsymbol{\Lambda}(\boldsymbol{q}) = \begin{bmatrix}\boldsymbol{\Lambda}_x & \boldsymbol{0}\\ \boldsymbol{0} & \boldsymbol{\Lambda}_n\end{bmatrix} \qquad \boldsymbol{\Gamma}(\boldsymbol{q},\dot{\boldsymbol{q}}) = \begin{bmatrix}\boldsymbol{\Gamma}_x & \boldsymbol{\Gamma}_{xn}\\ -\boldsymbol{\Gamma}_{xn}^T & \boldsymbol{\Gamma}_n\end{bmatrix} \ .$$

As above, for ease of presentation, the dependencies will be dropped in the remainder of the paper whenever this will not cause any ambiguity.

3. PROJECTION-BASED NULL SPACE COMPLIANCE CONTROL

In this section, first it is reviewed the original projection-based nullspace compliance control of Ott et al. (2008) and then the recent modification from Dietrich et al. (2016), which yields a passive closed-loop system. The controllers are reformulated and modified to facilitate the extension to the energy-based limit cycle control in Section 5.

3.1 Non-passive compliance control

The goal of the controller is to guarantee the fulfillment of the main task, i.e. $\boldsymbol{x}, \dot{\boldsymbol{x}} \to \boldsymbol{0}$ as $t \to \infty$, and the subordinate task of minimizing a potential energy function $U(\boldsymbol{q})$ within the nullspace of the main task. The classic controller in Ott et al. (2008) can be expressed as

$$\boldsymbol{\tau} = \boldsymbol{g} + \boldsymbol{J}_N^T\left(\begin{bmatrix}-\boldsymbol{D}_x & \boldsymbol{\Gamma}_{xn}\\ -\boldsymbol{\Gamma}_{xn}^T & -\boldsymbol{D}_n\end{bmatrix}\begin{bmatrix}\dot{\boldsymbol{x}}\\ \boldsymbol{v}\end{bmatrix} - \begin{bmatrix}\boldsymbol{K}_x\boldsymbol{x}\\ \boldsymbol{Z}\nabla U\end{bmatrix}\right) \ , \tag{7}$$

which consists of gravity compensation, a power-conserving compensation of the velocity-dependent couplings between the two tasks due to the Coriolis matrix and a spring-damper-like action for the execution of the tasks. The matrices $\boldsymbol{K}_x$, $\boldsymbol{D}_x \in \mathbb{R}^{m\times m}$ and $\boldsymbol{D}_n \in \mathbb{R}^{(n-m)\times(n-m)}$ are positive definite. If $U(\boldsymbol{q})$ is chosen such that it has a

[1] I.e. it fulfills the condition $\boldsymbol{J}(\boldsymbol{q})\boldsymbol{Z}^T(\boldsymbol{q}) = \boldsymbol{0}$.

[2] I.e. it fulfills the condition $\boldsymbol{J}(\boldsymbol{q})\boldsymbol{M}^{-1}(\boldsymbol{q})\boldsymbol{N}^T(\boldsymbol{q}) = \boldsymbol{0}$.

[3] Notice that using a dynamically consistent null space map the matrix $\boldsymbol{\Lambda}(\boldsymbol{q})$ is block diagonal.

constrained global minimum at $\boldsymbol{q} = \boldsymbol{q}_0$ on the submanifold defined by $\boldsymbol{x}(\boldsymbol{q}) = \boldsymbol{0}$, i.e.

$$U(\boldsymbol{q}) \geq 0,\ U(\boldsymbol{q}) = 0 \iff \boldsymbol{q} = \boldsymbol{q}_0, \quad \forall \boldsymbol{q} : \boldsymbol{x}(\boldsymbol{q}) = \boldsymbol{0} \tag{8a}$$

$$\boldsymbol{x}(\boldsymbol{q}_0) = \boldsymbol{0}\ , \tag{8b}$$

then the asymptotic stability of the equilibrium point $(\boldsymbol{q}, \dot{\boldsymbol{x}}, \boldsymbol{v}) = (\boldsymbol{q}_0, \boldsymbol{0}, \boldsymbol{0})$ is shown with the positive semi-definite Lyapunov functions

$$V_x = \frac{1}{2}\Big(\dot{\boldsymbol{x}}^T \boldsymbol{\Lambda}_x \dot{\boldsymbol{x}} + \boldsymbol{x}^T \boldsymbol{K}_x \boldsymbol{x}\Big) \tag{9}$$

$$V_n = \frac{1}{2}\boldsymbol{v}^T \boldsymbol{\Lambda}_n \boldsymbol{v} + U(\boldsymbol{q}) \tag{10}$$

via a conditional stability analysis. Nevertheless, choosing $S_1 = V_x + V_n$ as candidate storage function does not allow to show the passivity of the system with respect to the input $\boldsymbol{\tau}_e$ and output $\dot{\boldsymbol{q}}$. That is because

$$\dot{S}_1 = -\dot{\boldsymbol{x}}^T \boldsymbol{D}_x \dot{\boldsymbol{x}} - \boldsymbol{v}^T \boldsymbol{D}_n \boldsymbol{v} + \dot{\boldsymbol{x}}^T \boldsymbol{J}^{+T} \nabla U + \dot{\boldsymbol{q}}^T \boldsymbol{\tau}_e$$
$$\not\Rightarrow\ \dot{S}_1 \leq \dot{\boldsymbol{q}}^T \boldsymbol{\tau}_e\ ,$$

since the third term in $\dot{S}_1$ is not always non-positive. In Dietrich et al. (2016), a controller that leads to a passive closed-loop system has been proposed, which will be adapted and then modified in the following.

3.2 Passive compliance control

To obtain a passive system, the new storage function

$$S_2 = \frac{1}{2}\Big(\dot{\boldsymbol{x}}^T \boldsymbol{\Lambda}_x \dot{\boldsymbol{x}} + \boldsymbol{v}^T \boldsymbol{\Lambda}_n \boldsymbol{v} + \boldsymbol{x}^T \boldsymbol{K}_x \boldsymbol{x} + s^2\Big) + U(\hat{\boldsymbol{q}}) \tag{11}$$

is considered, in which $s \in \mathbb{R}$ is the level in the energy tank and $\hat{\boldsymbol{q}}$ is an auxiliary configuration variable. The dynamics of the newly introduced quantities are given by

$$\dot{\hat{\boldsymbol{q}}} = \begin{cases} \dot{\boldsymbol{q}} - \boldsymbol{K}_p\Big(\hat{\boldsymbol{q}} - \boldsymbol{q}\Big) & s > \epsilon \\ \boldsymbol{Z}^T \boldsymbol{v} & \text{else} \end{cases} \tag{12}$$

and

$$\dot{s} = \frac{1}{s}\Big(\dot{\boldsymbol{x}}^T \boldsymbol{D}_x \dot{\boldsymbol{x}} + \boldsymbol{v}^T \boldsymbol{D}_n \boldsymbol{v} + \tau_s\Big) \tag{13}$$

$$\tau_s = \begin{cases} \left[\Big(\hat{\boldsymbol{q}} - \boldsymbol{q}\Big)^T \boldsymbol{K}_p - \dot{\boldsymbol{x}}^T \boldsymbol{J}^{+T}\right] \nabla U(\hat{\boldsymbol{q}}) & s > \epsilon \\ \boldsymbol{0} & \text{else}\ , \end{cases} \tag{14}$$

where ϵ is a small positive value and $\boldsymbol{K}_p \in \mathbb{R}^{n \times n}$ is a positive definite matrix. The physical meaning is the following. The level in the tank keeps track of the energy dissipated by the system and the possible activity due to the coupling between the potential U and the main task. Activity in the system is allowed as long as the system has dissipated at least as much energy in the meantime, i.e. $s > \epsilon$. A higher initial level of the tank can be chosen to further increase the admissible level of activity in the system. When the tank gets empty, i.e. $s \leq \epsilon$, $\hat{\boldsymbol{q}}$ starts deviating from $\boldsymbol{q}$, meaning that the null space control performance is sacrificed in order to maintain passivity of the system. This is due to the fact that the modified control replaces $\nabla U(\boldsymbol{q})$ in (7) with $\nabla U(\hat{\boldsymbol{q}})$. Also, it is not difficult to show that with these choices the system is passive with respect to the external forces and the collocated velocities, since $\dot{S}_2 = \dot{\boldsymbol{q}}^T \boldsymbol{\tau}_e$.

4. AN IMPROVED PASSIVE COMPLIANCE CONTROL

Consider the following new candidate storage function

$$S_3 = \frac{1}{2}\Big(\dot{\boldsymbol{x}}^T \boldsymbol{\Lambda}_x \dot{\boldsymbol{x}} + \boldsymbol{v}^T \boldsymbol{\Lambda}_n \boldsymbol{v} + \boldsymbol{x}^T \boldsymbol{K}_x \boldsymbol{x}\Big) + s + U(\hat{\boldsymbol{q}})\ , \tag{15}$$

in which, with a slight abuse of notation and remembering the notation $\lfloor \boldsymbol{z} \rceil^p$ in Section 2, the new dynamics of the controller states are

$$\dot{\hat{\boldsymbol{q}}} = \begin{cases} \dot{\boldsymbol{q}} - \boldsymbol{K}_p \lfloor \hat{\boldsymbol{q}} - \boldsymbol{q} \rceil^{\frac{1}{2}} & s > 0 \\ \boldsymbol{Z}^T \boldsymbol{v} & \text{else} \end{cases} \tag{16}$$

and

$$\dot{s} = \dot{\boldsymbol{x}}^T \boldsymbol{D}_x \dot{\boldsymbol{x}} + \boldsymbol{v}^T \boldsymbol{D}_n \boldsymbol{v} + \tau_s + \tau_c \tag{17}$$

$$\tau_s = \begin{cases} \left[\Big(\boldsymbol{K}_p \lfloor \hat{\boldsymbol{q}} - \boldsymbol{q} \rceil^{\frac{1}{2}}\Big)^T - \dot{\boldsymbol{x}}^T \boldsymbol{J}^{+T}\right] \nabla U(\hat{\boldsymbol{q}}) & s > 0 \\ \boldsymbol{0} & \text{else} \end{cases} \tag{18}$$

$$\tau_c = \begin{cases} -K_s \tilde{S}_3 & s > 0\ \wedge\ \tilde{S}_3 > 0 \\ \boldsymbol{0} & \text{else}\ , \end{cases} \tag{19}$$

where $K_s > 0$, $\tilde{S}_3 = S_3 - S_d$ and constant $S_d \geq 0$. As before, assuming to have enough energy in the tank (i.e. $s > 0$), $\hat{\boldsymbol{q}}$ will converge to $\boldsymbol{q}$, but here the convergence happens in finite time, see Levant (1993), and not just exponentially. Additionally, the dynamics of the tank is not anymore numerically ill conditioned when the level approaches zero and (unlike in Section 3.2) no energy in the tank remains unused, i.e. $\epsilon = 0$. The role of S_d is to limit S_3 (and therefore the level in the tank) after physical interaction between the system and the environment. If not specifically taken into account, this value could get incremented at the end of an interaction and potentially grow unbounded, with possible undesired effects, since the level in the tank represents an upper bound for the allowed level of activity in the system. In Section 6, it is presented an example illustrating this phenomenon.

Differentiating S_3 with respect to time and using the control (7) in which $\nabla U(\hat{\boldsymbol{q}})$ replaces $\nabla U(\boldsymbol{q})$, one gets

$$\dot{S}_3 = \dot{\tilde{S}}_3 = \tau_c + \dot{\hat{\boldsymbol{q}}}^T \boldsymbol{\tau}_e \leq \dot{\boldsymbol{q}}^T \boldsymbol{\tau}_e\ . \tag{20}$$

Taking into account the dynamics (17), s is guaranteed to be always nonnegative, i.e $s \geq 0$. As a consequence, S_3 will be also always nonnegative and, given (20), it is a storage function with the closed-loop system being passive with respect to the input $\boldsymbol{\tau}_e$ and output $\dot{\boldsymbol{q}}$. From (20) and the expression of τ_c, it is clear that $\tilde{S}_3$ can increase only due to $\boldsymbol{\tau}_e$. For $\boldsymbol{\tau}_e = \boldsymbol{0}$, S_3 either decreases towards S_d (when $S_3 > S_d$) or it stays constant (when $S_3 \leq S_d$). Therefore, by adding τ_c in (17), the tank releases energy when the level is too high (release valve). It follows that a meaningful choice for S_d is $0 \leq S_d \leq S_3(t_0)$, where $S_3(t_0)$ is the initial value of the storage function. For values outside this interval, S_3 will reach the closest bound, i.e. 0 for $S_d < 0$ and $S_3(t_0)$ for $S_d > 0$. A choice which is always valid is for example to set S_d as the initial level in the tank, i.e. $S_d = s(t_0)$. In view of the energy flows within the system depicted in Fig. 2, it follows that as $t \to \infty$ then $\boldsymbol{q} \to \boldsymbol{q}_0$, $\boldsymbol{x}$, $\dot{\boldsymbol{x}}$, $\boldsymbol{v} \to \boldsymbol{0}$, and therefore $s \to s_\infty \leq S_d$, with $s_\infty < S_d$ if and only if energy has been removed during an interaction with the environment.

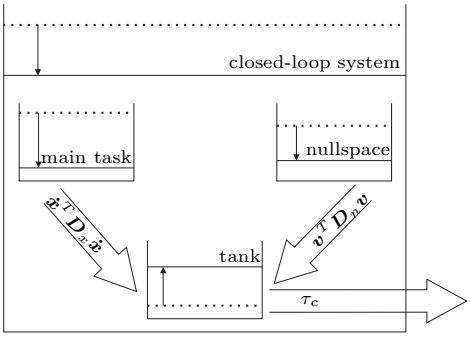

Fig. 2. Unidirectional energy flows within the closed-loop system. The dotted lines represent the energy at $t = t_0$, the continuous one the levels at $t_1 > t_0$.

5. PASSIVE ENERGY-BASED CONTROL

In this section, the previous results will be adapted to obtain an energy-based limit cycle controller. The first step in an energy-based control is the definition of an energy function. In view of (8) and the fact that $\boldsymbol{q}_0$ is an unique constrained minimum, the function

$$H = \frac{1}{2}\Lambda_n v^2 + U(\boldsymbol{q}) - U(\boldsymbol{q}_0) \tag{21}$$

is an energy function conditionally to the execution of the main task. Implicitly it has been assumed $v \in \mathbb{R}$, i.e. $m = n-1$. Garofalo et al. (2013); Garofalo and Ott (2016, 2017) show that this is a requirement when the controller is used for periodic motions, but it is not necessary when the energy-based control is used for compliance control. Defining $\tilde{H} = H - H_d$, with constant $H_d \geq 0$, the set

$$\mathcal{L}_d = \left\{ (\boldsymbol{q}, \dot{\boldsymbol{q}}) \mid \tilde{H} = 0,\ \boldsymbol{x} = \dot{\boldsymbol{x}} = \boldsymbol{0} \right\}$$

defines a closed orbit in the state space for $H_d > 0$ and a point for $H_d = 0$. As rule of thumb, one can choose U to influence the shape of the orbit and H_d for the size. In Garofalo et al. (2013), a controller is derived that satisfies the main task and renders $\mathcal{L}_d$ asymptotically stable for the whole system; the proof relying on a conditional stability analysis. For $H_d = 0$, the limit cycle collapses into an equilibrium point and the controller can be used for compliance control. Nevertheless, as in Section 3.1, the coupling between the main task and the energy regulation task did not allow to find a storage function to show the passivity of the closed-loop system w.r.t the input $\boldsymbol{\tau}_e$ and output $\dot{\boldsymbol{q}}$, or (equivalently) w.r.t the port

$$< \begin{bmatrix} \boldsymbol{f}_x \\ f_n \end{bmatrix}, \begin{bmatrix} \dot{\boldsymbol{x}} \\ v \end{bmatrix} > \qquad \text{with } \begin{bmatrix} \boldsymbol{f}_x \\ f_n \end{bmatrix} = \boldsymbol{J}_N^{-T} \boldsymbol{\tau}_e \ , \tag{22}$$

i.e. $\boldsymbol{f}_x$ and f_n are the components of the external torque $\boldsymbol{\tau}_e$ in the main and secondary task, respectively. Since for the energy control $\tilde{H}$ is relevant, the aim is to show the passivity using the output [4] $\tilde{H}v$ rather than v. Also, while the 1-DoF case has this passivity port, such property could not be shown in Garofalo et al. (2013) for the n-DoF case. Therefore, in the following a solution to overcome this problem is proposed.

Consider the control law with tank dynamics

$$\boldsymbol{\tau} = \boldsymbol{g} + \boldsymbol{J}_N^T \left(\begin{bmatrix} -\boldsymbol{D}_x & \boldsymbol{\Gamma}_{xn} \\ -\boldsymbol{\Gamma}_{xn}^T & -d_n \tilde{H} \end{bmatrix} \begin{bmatrix} \dot{\boldsymbol{x}} \\ v \end{bmatrix} - \begin{bmatrix} \boldsymbol{K}_x \boldsymbol{x} \\ \boldsymbol{Z} \nabla U(\hat{\boldsymbol{q}}) \end{bmatrix} \right) \tag{23}$$

$$\dot{s} = \dot{\boldsymbol{x}}^T \boldsymbol{D}_x \dot{\boldsymbol{x}} + d_n v^2 \tilde{H}_2^2 + \tilde{H}_2 \tau_s + \tau_c \ , \tag{24}$$

in which $\hat{\boldsymbol{q}}$ is obtained through (16) and τ_s, τ_c are given in (18)-(19), respectively. The key point in (23) is that the velocity feedback in the null space is proportional to the energy error. Therefore, energy can be both injected and removed from the system, guaranteeing the attainment of the desired value. Additionally, $U(\hat{\boldsymbol{q}})$ replaces $U(\boldsymbol{q})$ as in Section 4. Defining, $\tilde{S}_4 = S_4 - S_d$, $S_d \geq 0$ and

$$S_4 = \frac{1}{2}\Big(\dot{\boldsymbol{x}}^T \boldsymbol{\Lambda}_x \dot{\boldsymbol{x}} + \boldsymbol{x}^T \boldsymbol{K}_x \boldsymbol{x} + \tilde{H}^2 \Big) + s \ , \tag{25}$$

one obtains after lengthy, but simple derivations

$$\dot{H} = \dot{\tilde{H}} = -K_H v^2 \tilde{H} - \tau_s + v f_n \ , \tag{26}$$

$$\dot{S}_4 = \dot{\tilde{S}}_4 = \tau_c + \dot{\boldsymbol{x}}^T \boldsymbol{f}_x + \tilde{H} v f_n \leq \dot{\boldsymbol{x}}^T \boldsymbol{f}_x + \tilde{H} v f_n \ . \tag{27}$$

Therefore, S_4 is a storage function with the closed-loop system being passive with respect to the input $\begin{bmatrix} \boldsymbol{f}_x^T & f_n \end{bmatrix}^T$ and output $\begin{bmatrix} \dot{\boldsymbol{x}}^T & \tilde{H} v \end{bmatrix}^T$. The same considerations as in Section 4 hold here concerning the role of S_d and τ_c.

The previous results are summarized in the following

Proposition 1. Given the system (1) and the main task $\boldsymbol{x} = \boldsymbol{x}(\boldsymbol{q})$, let $\boldsymbol{K}_p$, $\boldsymbol{K}_x$, $\boldsymbol{D}_x$ be positive definite matrices, $\boldsymbol{K}_p$ also diagonal and K_s, $d_n > 0$. Additionally, consider the dynamics (16) and (24) with the energy functions (21) and (25). Then the control input (23) leads to

$$\begin{aligned} &\boldsymbol{\Lambda}_x \ddot{\boldsymbol{x}} + \Big(\boldsymbol{\Gamma}_x + \boldsymbol{D}_x \Big) \dot{\boldsymbol{x}} + \boldsymbol{K}_x \boldsymbol{x} = \boldsymbol{f}_x \\ &\Lambda_n \dot{v} + \Big(\boldsymbol{\Gamma}_n + d_n \tilde{H}_2 \Big) v + \boldsymbol{Z} \nabla U(\hat{\boldsymbol{q}}) = f_n \ , \end{aligned} \tag{28}$$

which is passive with input $\begin{bmatrix} \boldsymbol{f}_x^T & f_n \end{bmatrix}^T$, output $\begin{bmatrix} \dot{\boldsymbol{x}}^T & \tilde{H} v \end{bmatrix}^T$ and storage function S_4.

6. VALIDATION

The controller proposed in Section 5 is evaluated first in simulation and then in an experiment. The simulation is used to compare it with the control law in Section 3.2. Therefore, the desired energy value is set to $H_d = 0$ in order to solve a regulation task. On the other hand, in the experiment this value is set to $H_d = 2\,\mathrm{J}$ to show the capability of the controller to generate a periodic motion.

6.1 Simulations

The planar robot in Fig. 3 is considered in the simulation. The specifications of the robot, the controller parameters and the definition of the test case are taken from Dietrich et al. (2016). The main task requires the robot to reach a desired position of the end-effector, while the secondary task specifies the position for the first joint and the end-effector orientation. The desired values are chosen in such a way that the secondary task is partially in conflict with the main one. Additionally, at $t = 1\,\mathrm{s}$ a sinusoidal external force at the end-effector is applied along the horizontal position. The duration of the signal is 1 s and it has a frequency of 3 Hz and amplitude of 60 N.

Fig. 4 collects the results of three simulations. In two of them, it was used the controller of Section 3.2. As in

[4] This implies some robustness to f_n after convergence, since f_n does not change the storage function for $\tilde{H} = 0$.

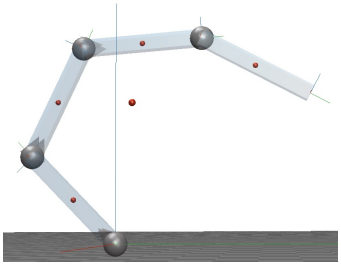

Fig. 3. Planar robot with 4 revolute joints used in the simulation in its initial configuration. Each link has a point mass of 1 kg, placed in the middle of the link of length 0.5 m.

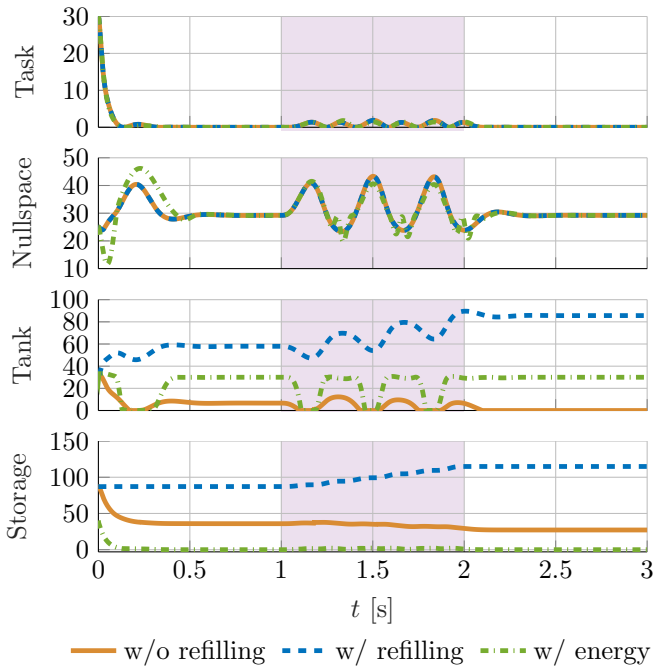

Fig. 4. Energy values obtained during three different simulations. In the shaded area, an external force is acting at the end-effector.

Dietrich et al. (2016), once all the dissipated energy is redirected towards the tank, while the tank is not refilled at all in the other. The controller (23) is used in the last simulation. The main task is executed perfectly in all cases, while the error of the secondary task cannot go to zero due to the interference with the main one. While the performance of the robot are similar, a different state is reached for the tank, which can effect the future evolution of the system. Without refilling the tank gets empty. In contrast, the level grows due to the external force using the refilling. Finally, thanks to the release valve the level in the tank goes back to its initial value.

6.2 Experiment

The control law (23) is evaluated in an experiment with the humanoid robot TORO, which is described in Englsberger et al. (2014).

Desired configuration and constraint function In this example, the constraint submanifold is given directly in joint space. TORO is using its legs to maintain balance, while the 12 joints of the arms are forced on a submanifold defined by the constraint functions

$$x_i(\boldsymbol{q}) = q_i - q_{d_i} - q_{c_i} \qquad i = 2, \ldots, 12 \ , \tag{29}$$

where $\boldsymbol{q}_c$ is used to couple the elbow joint of the right arm to the first joint of the shoulder of the same arm, i.e. $q_{c_4} = 5q_1$ while the rest of the entries are zero. Finally $\boldsymbol{q}_d$ is chosen to be the desired configuration shown in Fig. 5. It is worth to notice that choosing $q_{d_1} = 0$, then the condition $\boldsymbol{x}(\boldsymbol{q}_d) = \boldsymbol{0}$ is satisfied.

Fig. 5. TORO in the handshake configuration.

Potential function A simple choice for the virtual potential is given by

$$U(\boldsymbol{q}) = \frac{1}{2} k_n \left\| \boldsymbol{q} - \boldsymbol{q}_d \right\|^2 \ , \tag{30}$$

where $k_n = 40\,\mathrm{Nm/rad}$. $U(\boldsymbol{q})$ so defined is clearly positive definite for $\boldsymbol{x}(\boldsymbol{q}) = \boldsymbol{0}$ and has its minimum at $\boldsymbol{q}_d$.

Results Given the definition of $\boldsymbol{x}(\boldsymbol{q})$, the result will be a handshaking motion in which the first shoulder joint works as limit cycle generator with the elbow joint coupled to it. The remaining ones will keep the desired position. Fig. 6 shows the measured H, for H_d going from 0 to 2 J and back. This initiates and stops the handshaking motion.

Discussion In Fig. 6 the energy oscillates around its desired value, although convergence was theoretically expected. Measurement noise, flexibility of the structure, the movement of the lower body which is not fixed to the floor and model uncertainties are a possible cause for this phenomenon. The mismatch between the real model and the one used by the controller and the limitations of the balancing controller are supposed to be the main reason for the oscillations in the recorded signal. The behavior can be reproduced in simulation when using an incorrect model for the controller and disappears when the model is perfectly known. The experiment gives the opportunity to test the robustness of the proposed approach. Although it was not formally shown, the behavior results to be periodic even if the energy error does not converge exactly to zero, showing that the effect of the model uncertainty is a distortion of the expected attractive closed orbit.

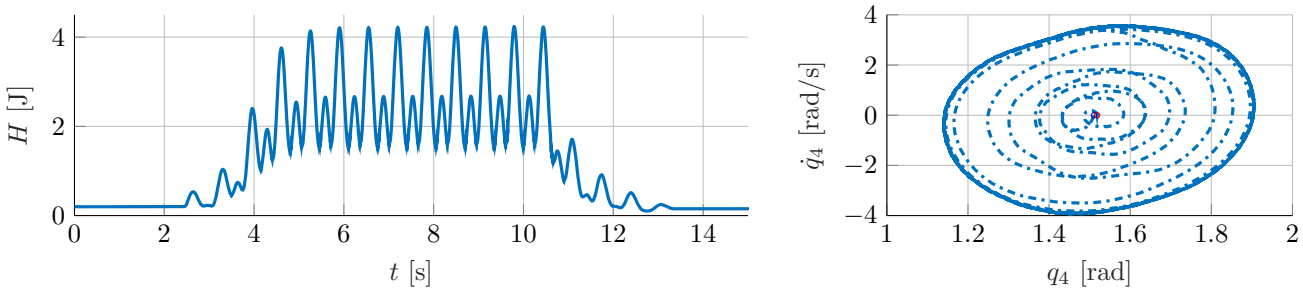

Fig. 6. Results of the experiment with TORO. Left: energy plot. Right: phase plot for the elbow joint.

7. CONCLUSION

The paper walks the reader through the derivation of a novel control law for passivation of energy-based limit cycle control. The method is similar to the passive projection-based null space compliance control, but it extends it in different ways. A release valve is added to the energy tank to limit the energy that can accumulate during interaction, as well as modification that improve the convergence rate and numerical conditioning. Finally, an important extension consist in the ability to use the controller for generating periodic behaviors, i.e. limit cycles. These techniques have been used recently for physical human-robot interaction and locomotion tasks, although passivity with respect to the external forces and collocated velocities had not been taken into account. Therefore, the proposed method represents a key extension for all these applications in which the passivity of the system is a paramount requirement to guarantee the stability, robustness and safety during the interactions.

REFERENCES

Canudas-de-Wit, C., Espiau, B., and Urrea, C. (2002). Orbital stabilization of underactuated mechanical systems. In *Triennial World Congress of the International Federation of Automatic Control*, 893–898. Barcelona, Spain.

Dietrich, A., Ott, C., and Stramigioli, S. (2016). Passivation of projection-based null space compliance control via energy tanks. *IEEE Robotics and Automation Letters (RA-L)*, 1(1), 184–191.

Duindam, V. and Stramigioli, S. (2003). Passive asymptotic curve tracking. In *Proceedings of the IFAC Workshop on Lagrangian and Hamiltonian Methods for Nonlinear Control*, 229–234. Seville, Spain.

Englsberger, J., Werner, A., Ott, C., Henze, B., Roa, M.A., Garofalo, G., et al. (2014). Overview of the torque-controlled humanoid robot TORO. In *IEEE/RAS Int. Conf. on Humanoid Robots*, 916–923. Madrid, Spain.

Garofalo, G. and Ott, C. (2016). Limit cycle control using energy function regulation with friction compensation. *IEEE Robotics and Automation Letters (RA-L)*, 1(1), 90–97.

Garofalo, G. and Ott, C. (2017). Energy based limit cycle control of elastically actuated robots. *IEEE Trans. on Automatic Control*, 62(5), 2490–2497.

Garofalo, G. and Ott, C. (2019). Repetitive jumping control for biped robots via force distribution and energy regulation. In F. Ficuciello, F. Ruggiero, and A. Finzi (eds.), *Human Friendly Robotics, 10th International Workshop*, Springer Proceedings in Advanced Robotics (SPAR), 29–45. Springer.

Garofalo, G., Ott, C., and Albu-Schäffer, A. (2012). Walking control of fully actuated robots based on the bipedal SLIP model. In *IEEE Int. Conf. on Robotics and Automation (ICRA)*, 1999–2004. Saint Paul, USA.

Garofalo, G., Ott, C., and Albu-Schäffer, A. (2013). Orbital stabilization of mechanical systems through semidefinite Lyapunov functions. In *American Control Conference (ACC)*, 5735–5741. Washington DC, USA.

Geyer, H., Seyfarth, A., and Blickhan, R. (2006). Compliant leg behavior explains basic dynamics of walking and running. *Proceedings of the Royal Society B*, 273, 2861–2867.

Levant, A. (1993). Sliding order and sliding accuracy in sliding mode control. *International Journal of Control*, 58(6), 1247–1263.

Li, P.Y. and Horowitz, R. (2001). Passive velocity field control (pvfc). *IEEE Trans. on Automatic Control*, 46(9), 1346–1371.

McGeer, T. (1990). Passive dynamic walking. *Int. Journal of Robotics Research*, 9, 62–82.

Ott, C., Kugi, A., and Nakamura, Y. (2008). Resolving the problem of non-integrability of nullspace velocities for compliance control of redundant manipulators by using semi-definite Lyapunov functions. In *IEEE Int. Conf. on Robotics and Automation (ICRA)*, 1456–1463. Pasadena, USA.

Park, J., Chung, W., and Youm, Y. (1999). On dynamical decoupling of kinematically redundant manipulators. In *IEEE/RSJ International Conference on Intelligent Robots and Systems*, 1495 –1500.

Petrič, T., Gams, A., Žlajpah, L., and Ude, A. (2014). Online learning of task-specific dynamics for periodic tasks. In *IEEE/RSJ Int. Conf. on Intelligent Robots and Systems (IROS)*, 1790–1795. Chicago, USA.

Stramigioli, S. (2015). Energy-aware robotics. In M.K. Camlibel, A.A. Julius, R. Pasumarthy, and J.M. Scherpen (eds.), *Mathematical Control Theory I: Nonlinear and Hybrid Control Systems*, Lecture Notes in Control and Information Sciences. Springer International Publishing, Switzerland.

Taniguchi, M. and Fujimoto, K. (2009). Asymptotic path following and velocity control of port-Hamiltonian systems. In *European Control Conference (ECC)*, 236 – 241. Budapest, Hungary.

Westervelt, E.R., Grizzle, J.W., Chevallereau, C., Choi, J.H., and Morris, B. (2007). *Feedback Control of Dynamic Bipedal Robot Locomotion*. CRC Press.